Effect of anisotropy on stress-induced electrical potentials in bovine bone using ultrasound irradiation

S. Matsukawa,[1] T. Makino,[1] S. Mori,[1] D. Koyama,[1] S. Takayanagi,[2] K. Mizuno,[3] T. Yanagitani,[4] and M. Matsukawa[1,a)]

[1]*Laboratory of Ultrasonic Electronics, Doshisha University, 1-3, Tatara Miyakodani, Kyotanabe, Kyoto 610-0321, Japan*
[2]*Graduate School of Engineering, Nagoya Institute of Technology, Gokiso cho, Showa-ku, Nagoya 466-8555, Japan*
[3]*Underwater Technology Collaborative Research Center, Institute of Industrial Science, The University of Tokyo, 4-6-1, Komaba, Meguro-ku, Tokyo 153-8505, Japan*
[4]*Department of Electrical Engineering and Bioscience, Waseda University, 3-4-1, Okubo, Shinjuku, Tokyo 169-8555, Japan*

(Received 13 December 2016; accepted 21 March 2017; published online 3 April 2017)

The bone fracture healing mechanism of the low-intensity pulsed ultrasound technique is not yet clearly understood. In our previous study, the electrical potentials induced in bone were successfully measured by focusing on piezoelectricity in the MHz range. Bone is composed of collagen and hydroxyapatite and has strong anisotropy. The purpose of this study is to investigate the effects of bone anisotropy on the electrical potentials induced by ultrasound irradiation. For this study, ultrasound bone transducers were fabricated using cortical bovine bone plates as piezoelectric devices. An ultrasound of 7.4 $kPa_{peak\text{-}peak}$ (i.e., the peak-to-peak pressure value) was used to irradiate the side surface of each bone plate. Electrical potentials induced in the bone plate were then measured by varying the wave propagation direction in the plate. The peak-to-peak values of these ultrasonically induced electrical potentials were found to vary with changes in the ultrasound propagation direction in the bone sample. The potential was maximized at an inclination of approximately 45° to the bone axis but was minimized around the three orthogonal directions. These maxima and minima ranged from 28 to 33 $\mu V_{peak\text{-}peak}$ and from 5 to 12 $\mu V_{peak\text{-}peak}$, respectively. Additionally, our ultrasound results indicated a change in polarity due to bone anisotropy in the MHz range. *Published by AIP Publishing.* [http://dx.doi.org/10.1063/1.4979599]

Bone growth is promoted by ultrasound irradiation.[1] Recently, the low intensity pulsed ultrasound (LIPUS) technique was used to aid in healing of bone fractures. The LIPUS technique typically uses pulsed 1.5 to 3 MHz ultrasound for 5 to 20 min per day, which results in bone fracture healing times being accelerated by approximately 20%–30%.[2,3] While there have been several reports of *in vivo* experiments using LIPUS in the literature, the primary mechanism of the LIPUS technique is not yet fully understood.[4,5] Padilla reported that the biological response to LIPUS is complex and that different cell types respond to ultrasound irradiation through various pathways.[6]

Several researchers have studied bone growth from the electrical perspective. One previous study reported that application of mechanical stress at low frequencies induced electrical potentials in bone.[7] Shamos and Lavine proved that these electrical potentials are related to the bone remodeling mechanism.[8] These studies that used low frequency mechanical stress indicated that there were two main mechanisms to induce electrical potentials in bone: the piezoelectricity and the streaming potential. The streaming potential is induced via an interaction between the liquid and solid phases of the complex wet bone structure.[9] Anderson and Eriksson found that the potentials induced in wet bones were higher than those induced in dry bones at low frequencies, thus implying the generation of a streaming potential.[10] Qin *et al.* quantitatively measured the time scale relaxation behavior of both intramedullary pressure and the streaming potentials *in vivo*.[11] Additionally, Fukada and Yasuda linked empirical evidence of stress-induced electrical potentials in bone to piezoelectricity and hypothesized that the piezoelectricity in bone had no relationship with bone viability.[7] The existence of piezoelectricity in decalcified bone was also confirmed.[12,13] The origin of this effect is believed to be related to the piezoelectricity of collagen molecules and hydroxyapatite (HAp) in bone. In decalcified bone, we can expect piezoelectricity due to collagen only. The crystallographic symmetry of collagen, which is supposed to be of hexagonal C_6-type, is largely responsible for the piezoelectricity in bone.[14] Zhang *et al.* reported that the piezoelectric response of extracted collagen is much higher than that of HAp.[15] However, the conventional LIPUS technique uses MHz-range ultrasound, and most studies have tested bone piezoelectricity at low frequencies ranging up to several kHz. To clarify the ultrasound-based bone healing mechanism, it is important to investigate the stress-induced electrical potential that occurs in the MHz range.

To evaluate stress-induced electrical potentials in bone quantitatively in the MHz range, we fabricated ultrasound transducers using bones as piezoelectric devices in our previous work. Based on the observation of waveforms detected using handmade bone transducers, we confirmed the

a)E-mail: mmatsuka@mail.doshisha.ac.jp

existence of the piezoelectric effect in this range.[16] The stress-induced electrical potentials of these bone transducers were almost 1/1000 of that of a polyvinylidene fluoride (PVDF) film transducer (10 mm diameter, flat type; handmade). Additionally, these stress-induced electrical potentials could be observed in wet bone. The relationship between these electrical potentials and the bone sample microstructure was also investigated.[17] However, the analysis of ultrasound propagation in bone is very difficult because of the complex shape, anisotropy, and heterogeneity of bone. Therefore, to provide better understanding of the mechanism that relates ultrasound-induced electrical potentials to bone healing, we focused on bone anisotropy.

In this work, we have experimentally observed the effects of bone anisotropy on the electrical potentials induced by ultrasonic irradiation. The study focused specifically on the relationship between the stress-induced electric potential and ultrasound propagation direction.

An example of the sample preparation process is shown in Fig. 1. Right femora were obtained from bovines aged from 31 to 40 months. Cortical bone samples were extracted from anterior sections of the mid-shafts of the femora and were then processed into circular plates. We fabricated three sample types, namely, types A, B, and C; these types were circular plates that were cut normal to the radial direction of the bone axis, normal to the direction tangential to the bone axis, or normal to the bone axis, respectively. Sample diameters ranged from 10.5 to 11.5 mm, while the sample thickness was 3.00 ± 0.01 mm. Ultrasound bone transducers were then fabricated to act as receivers, using the bone plates as piezoelectric materials. The active area diameter of each of these transducers was 10.0 mm.

The cortical bone, which is composed of inorganic HAp and organic type I collagen, is both hard and dense. These two components are highly orientated along the bone axis, which produces a strong anisotropy.[18] The longitudinal wave velocity in cortical bone is dependent on the propagation angle relative to the long axis of the bone and has its maximum value in the axial direction.[18–20] The longitudinal wave propagation velocities in these bone samples varied relative to the propagation direction: velocities in the axial direction ranged from 4180 m/s (type B) to 4265 m/s (type A), while those in the radial direction ranged from 3389 m/s (type B) to 3448 m/s (type C), and those in the tangential direction ranged from 3630 m/s (type C) to 3760 m/s (type A). These values agreed well with previously reported results.[18,19]

The electrical potentials in the bones were measured using a conventional immersion ultrasonic pulse system.[19] A PVDF focused transducer (diameter: 20 mm; focal length: 40 mm; custom-made by Toray Engineering, Tokyo, Japan) was used as the transmitter, and a handmade bone transducer was used as the receiver. The focal region diameter was 3 mm. The bone sample thickness was also 3 mm. The effects of multiple reflections in the bone seem to be small because the ultrasound irradiated the side surface of the circular plate. In the experimental system, the transmitter and the receiver were set such that they were crossed at right angles in degassed water, as shown in Fig. 2(a). The distance from the side surface of the bone sample to the transmitter was 40 mm. A function generator (33250A; Agilent Technologies, Santa Clara, CA) delivered an electrical pulse (step signal, 70 $V_{peak\text{-}peak}$) to the transmitter, which was then converted into a short ultrasound pulse. We did not use a pulsar system. The short ultrasound pulse was produced using a step input signal at the initial part of a square pulse. This ultrasound pulse was then used to irradiate the bone transducer's side surface. Figure 2(b) shows a received waveform that was measured using a PVDF transducer at a distance of 40 mm from the transmitter (PVDF-focused transducer). A very short pulse was realized. The peak-to-peak waveform value observed at the focus point was approximately 38 $mV_{peak\text{-}peak}$ (7.4 $kPa_{peak\text{-}peak}$), and the wave frequency was around 760 kHz. The induced electrical potential signal was then amplified by 40 dB using a preamplifier (BX-31A; NF, Yokohama, Japan) and observed using an oscilloscope (DPO3054; Tektronix, Beaverton, OR). Measurements were performed at each sample rotation angle θ from 0° to 360°. In the case where $\theta = 0°$, the ultrasound propagates along the axial direction. We measured the electrical potentials using electrodes in the upper and lower surfaces.

Figure 3 shows the waveforms observed using transducer type A. Here, 0° is the bone axis direction. The stress-induced electric potentials varied with ultrasound propagation direction in the bone sample. These potentials were maximized

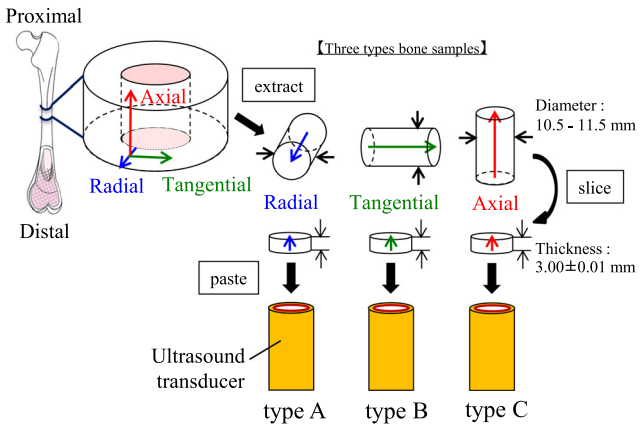

FIG. 1. Bone plate sample fabrication process. Bone cylinders obtained from the mid-shaft of a bovine femur were oriented parallel to the bone radial (type A), tangential (type B), or axial (type C) directions.

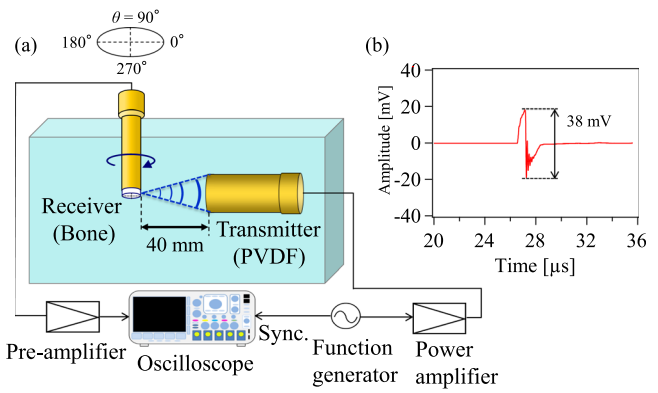

FIG. 2. Diagram of the experimental system. (a) The transmitter and receiver were set to be crossed at right angles in degassed water. The bone sample's side surface was located 40 mm from the transmitter (i.e., at the transmitter's focal length). Ultrasound measurements were taken at each rotation angle θ from 0° to 360°. (b) Ultrasound waveform radiated by the PVDF transducer at the focus point.

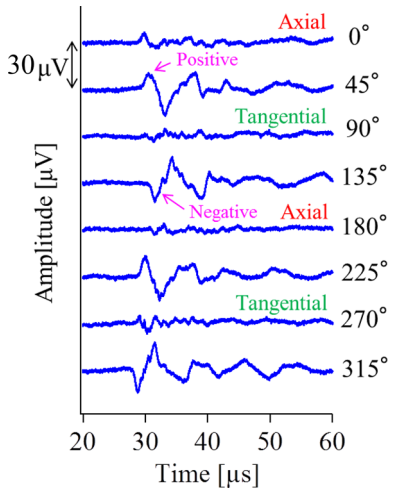

FIG. 3. Waveforms observed for bone transducer type A. 0° and 180° indicate the bone axial directions. 90° and 270° are tangential to the bone axis.

when the ultrasound propagated in an off-axis direction. The peak-to-peak stress-induced electric potential values were 10 $\mu V_{peak\text{-}peak}$ at $\theta = 0°$ and 28 $\mu V_{peak\text{-}peak}$ at $\theta = 45°$. These peak-to-peak values were defined as the amplitude difference between the first positive (or negative) peak and the second negative (or positive) peak of the stress-induced electric potentials. The frequency of the first wave in the off-axis direction ranged from 200 to 250 kHz, which was lower than the wave frequencies observed using the PVDF transducer. In this experiment, ultrasound was used to irradiate the side surfaces of the bone transducer. During ultrasound propagation across the transducer surface, the observed waveform frequency apparently decreased because the wavelength is smaller than the transducer diameter.

The wavefront polarity also varied with changes in the ultrasound propagation direction in the bone sample. In a previous study, Anderson and Eriksson reported that the piezoelectric constants of bone at low frequencies are $d_{12} = 0.083$ pC/N and $d_{13} = -0.037$ pC/N, reflecting bone's anisotropy.[10] Our ultrasound results also indicated a polarity change due to bone anisotropy in the MHz range.

The stress-induced electrical potentials for transducer types A, B, and C were measured at each 10° rotation. Figure 4 shows the relationship between the polarity and the peak-to-peak values of the stress-induced electrical potential waveforms and ultrasound propagation direction. Figure 4(a) shows the results for transducer type A. In this figure, the wave polarity was positive from 0° to 90° and from 180° to 270° and was negative from 100° to 170° and from 280° to 350°. Additionally, the peak-to-peak values reached maxima at approximately 30°, 135°, 240°, and 320° and minima at approximately 90°, 180°, 270°, and 350°. These maxima and minima ranged from 28 to 33 $\mu V_{peak\text{-}peak}$ and from 5 to 12 $\mu V_{peak\text{-}peak}$, respectively. By focusing on these figures, we determined that the directions of these minima and maxima were slightly inclined from $\theta = 0°$ or 45°. We then measured the HAp orientation using the X-ray diffraction technique (X-Pert Pro MRD; Philips, Hamburg, Germany). The HAp orientation in the sample was inclined by approximately 3° from the bone axis, which corresponded well to the results of Nakatsuji *et al.*[19] Therefore, the results in Fig. 4 indicate the possibility that the minimum output angle is not 0°. Fukada reported that the piezoelectric effect did not occur in bone when the sample was pressured at an incline of approximately 10° from the bone axis. Fukada also measured the HAp orientation of the sample to be inclined at approximately 10° to the bone axis.[7] Our results have thus possibly come from the HAp inclination and the collagen orientation.

Figure 4(b) shows the results that were measured using transducer type B. The polarities also changed, and the peak-to-peak values reached maxima at approximately 30°, 130°, 230°, and 310° and minima at approximately 90°, 180°, 270°, and 350°. These maxima and minima ranged from approximately 28 to 33 $\mu V_{peak\text{-}peak}$ and approximately from 5 to 7 $\mu V_{peak\text{-}peak}$, respectively. These results showed similar tendencies to those shown in Fig. 4(a). Finally, Fig. 4(c) shows the results measured using transducer type C. The polarities also changed in this case. However, the peak-to-peak values in Fig. 4(c) were smaller than those in Figs. 4(a) and 4(b). These values ranged from 4 to 16 $\mu V_{peak\text{-}peak}$, and the anisotropic behavior in this plane was thus weak.

Yamato *et al.* reported that cortical bone shows its highest elasticity and velocity in the axial direction.[18] In this study, the sample velocities were high in the axial direction but low in the radial and tangential directions. However, the stress-induced electrical potentials in the bone samples were small in the three orthogonal directions but high at an angle of approximately 45° to the bone axis. Fukada *et al.* reported that the polarity and magnitude of the charge that appeared on the cubic bone sample's surface differed depending on the direction in which the pressure was applied at 2 kHz.

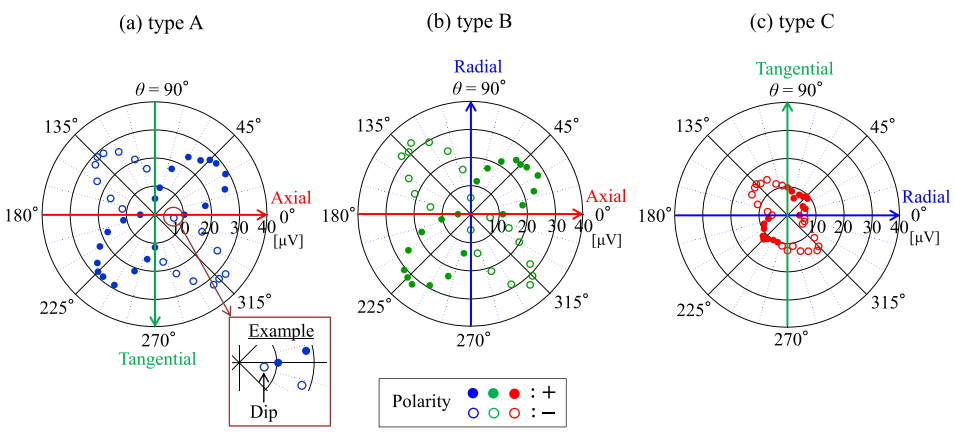

FIG. 4. Relationship between the polarity and peak-to-peak values of stress-induced electric potentials and the ultrasound irradiation directions. Results were measured for (a) type A, (b) type B, and (c) type C transducers.

This phenomenon arose in human and in bovine bones and in Achilles tendons (both bovine and horse), which are mainly composed of collagen fibers. The charge magnitude was higher when the pressure was directed at an angle of approximately 50° to the bone axis.[7,14] Our results also indicated a similar tendency for the ultrasound irradiation. Additionally, Fukada *et al*. calculated that $d_{13} = d_{23} = 0$ and concluded that the crystallographic symmetry in these collagen crystals was likely to be hexagonal C_6. In our results, d_{13} is the piezoelectric constant at 0° in transducer type A, and d_{23} is the corresponding constant at 0° in transducer type B. However, these constants had nonzero values. The data presented here imply the possibility of other crystallographic symmetries in bones.

In this study, we investigated the effects of bone anisotropy on stress-induced electrical potentials in bone. The polarities and amplitudes of these stress-induced electrical potentials varied with the ultrasound propagation direction in each bone sample. The results indicate that there is an optimal ultrasound radiation direction that can be used to induce similar electrical potentials *in vivo*. In this study, the effects of ultrasound attenuation in bone[21,22] were not investigated. We also need to investigate the refraction and the propagation path of ultrasound in the sample when it enters the side surface of the bone. These aspects will be addressed as part of our future studies.

Part of this work was supported by the Medical Ultrasound Center at Doshisha University.

[1]L. R. Duarte, Arch. Orthop. Trauma Surg. **101**, 153 (1983).
[2]H. Lu, L. Qin, K. Lee, W. Cheung, K. Chan, and K. Leung, Biochem. Biophys. Res. Commun. **378**(3), 569 (2009).
[3]T. Nakamura, S. Fujihara, K. Yamamoto-Nagata, T. Katsura, T. Inubushi, and E. Tanaka, Ann. Biomed. Eng. **39**(12), 2964 (2011).
[4]C. A. M. Xavier and L. R. Duarte, Rev. Bras. Orthop. **18**, 73 (1983).
[5]J. D. Heckman, J. P. Ryaby, J. McCabe, J. J. Frey, and R. F. Kilcoyne, J. Bone Joint Surg. **76-A**, 26 (1994).
[6]F. Padilla, Ultrasonics **54**, 1125–1145 (2014).
[7]E. Fukada and I. Yasuda, J. Phys. Soc. Jpn. **12**, 1158 (1957).
[8]M. H. Shamos and L. S. Lavine, Clin. Orthop. **35**, 177 (1964).
[9]W. Starkebaum, S. R. Pollack, and E. Korostoff, J. Biomed. Mater. Res. Part A **13**, 729 (1979).
[10]J. C. Anderson and C. Eriksson, Nature **227**, 491 (1970).
[11]Y. Qin, W. Lin, and C. Rubin, Ann. Biomed. Eng. **30**, 693 (2002).
[12]A. A. Marino, R. O. Becker, and S. C. Soderholm, Calcif. Tissue Res. **8**, 177 (1971).
[13]L. Bassett, R. J. Pawluk, and R. O. Becker, Nature **204**, 652 (1964).
[14]E. Fukada and I. Yasuda, Jpn. J. Appl. Phys., Part 1 **3**, 117 (1964).
[15]Y. Zhang, A. A. Gandhi, J. Zeglinski, M. Gregor, and S. A. M. Tofail, IEEE Trans. Dielectr. Electr. Insul. **19**, 1151 (2012).
[16]M. Okino, S. Coutelou, K. Mizuno, T. Yanagitani, and M. Matsukawa, Appl. Phys. Lett. **103**, 103701 (2013).
[17]H. Tsuneda, S. Matsukawa, S. Takayanagi, K. Mizuno, T. Yanagitani, and M. Matsukawa, Appl. Phys. Lett. **106**, 073704 (2015).
[18]Y. Yamato, M. Matsukawa, T. Yanagitani, K. Yamazaki, H. Mizukawa, and A. Nagano, Calcif. Tissue Int. **82**, 162 (2008).
[19]T. Nakatsuji, K. Yamamoto, D. Suga, T. Yanagitani, M. Matsukawa, K. Yamazaki, and Y. Matsuyama, Jpn. J. Appl. Phys., Part 1 **50**, 07HF18 (2011).
[20]K. Yamamoto, T. Nakatsuji, Y. Yaoi, Y. Yamato, T. Yanagitani, M. Matsukawa, K. Yamazaki, and Y. Matsuyama, Ultrasonics **52**, 377 (2012).
[21]M. Sasso, G. Haïat, Y. Yamato, S. Naili, and M. Matsukawa, Ultrasound Med. Biol. **33**(12), 1933 (2007).
[22]M. Sasso, G. Haïat, Y. Yamato, S. Naili, and M. Matsukawa, J. Biomech. **41**, 347 (2008).